



Glucose utilization in the inferior cerebellar vermis and ocular myoclonus

Abstract—In a patient with symptomatic ocular myoclonus, the authors observed the regional cerebral metabolic rate of glucose use (rCMRglu) before and after successful treatment with clonazepam. Even after the symptoms resolved, the rCMRglu in the hypertrophic olive increased persistently, whereas that in the inferior cerebellar vermis contralateral to the hypertrophic olive decreased. The inferior cerebellar vermis, belonging to the vestibulocerebellar system, may be associated with the generation of symptomatic ocular myoclonus.

NEUROLOGY 2006;67:131–133

Y. Yakushiji, MD; R. Otsubo, MD; T. Hayashi, MD; K. Fukuchi, MD; N. Yamada, MD; Y. Hasegawa, MD; and K. Minematsu, MD

Symptomatic ocular myoclonus is a disorder in which there are spontaneous, rhythmic, pendular oscillations of the eyes. It can occur alone or may be accompanied by myoclonic movements in other muscles derived from the embryonal branchial arches, particularly the palate,¹ known as branchial myoclonus. The region that generates abnormal myoclonic activity has not been localized. A previous study using PET disclosed an increase of regional cerebral glucose use (rCMRglu) throughout the medulla in patients with symptomatic palatal or oculopalatal myoclonus,² leading to the hypothesis that hyperactivity of the inferior olive may produce symptomatic branchial myoclonus. However, the mechanism that leads to such symptoms remains a matter of discussion. To further clarify this issue, using PET with F-18 fluorodeoxyglucose (FDG-PET), we investigated the topographic distribution of rCMRglu changes before and after successful treatment of symptomatic ocular myoclonus.

Case report. An 80-year-old hypertensive woman, who had had a pontine tegmental hemorrhage 5 months previously, was referred to our hospital because of ocular oscillations. On admission, oculomotor examination showed a right-sided one-and-a-half syndrome and involuntary rhythmic continuous vertical ocular movements in both eyes that were unaffected by caloric testing. Palatal myoclonus and other abnormal involuntary movements were absent.

Brain T2-weighted MRI, performed on admission, revealed an old, small hemorrhage on the right side of the pontine tegmentum and the hypertrophic olive on the right side of the medulla (figure 1, A and B). Electronystagmography (ENG), performed on the day just before treatment (day 0), showed a rhythmic, pendular, vertical ocular myoclonus at 2 to 3 cycles/second (figure 2A). The amplitude of the ocular myoclonus was larger on the left than on the right. On the same day, we performed a FDG-PET scan after the IV injection of 5 mCi of FDG, and we found increased uptake of FDG on the right side of the ventral medulla (figure 2B). Using SPM99 software, we compared the FDG accumulation image to the T2-weighted magnetic resonance image and confirmed that the region with the increased FDG uptake corresponded to the hypertrophic olive region (figure 2C).

To treat the patient's symptomatic ocular myoclonus, clonazepam was started at a dose of 0.5 mg/day. As the clonazepam dosage was increased, the symptomatic ocular myoclonus gradually decreased and almost disappeared on day 7 when the clonazepam dosage was 2 mg/day and no severe side effects were noted (figure 2D). After obtaining informed consent from the patient, on day 7 we performed a follow-up FDG-PET and found that the increased rCMRglu in the hypertrophic olive region remained unchanged (figure 2, E and F). To investigate any change in the distribution of FDG uptake, we compared FDG accumulation images taken before and after treatment and proportionally scaled the whole brain activity of FDG uptake to 100. Next, we subtracted the scaled images (day 0 minus day 7) and smoothed the resulting image using a gaussian filter with a resolution of 8 mm to generate a difference image based on a unit of percent global value. The difference image revealed that the highest decrease in the normalized rCMRglu was located in the inferior cerebellar vermis (−25%) contralateral to the hypertrophic olive (figure 3), whereas no significant decrease (less than −5%) was found in the hypertrophic olive that showed increased activity on the first FDG-PET scan. No other regions showed a larger than 5% difference in FDG uptake.

Discussion. Symptomatic ocular myoclonus occasionally follows brainstem lesions and is a major ac-

From the Cerebrovascular Division, Department of Medicine (Y.Y., R.O., Y.H., K.M.), Department of Investigative Radiology, Advanced Medical Engineering Center, Research Institute (T.H.), and Department of Radiology and Nuclear Medicine (T.H., K.F., N.Y.), National Cardiovascular Center, Osaka, Japan. Dr. Yakushiji is currently with the Division of Neurology, Department of Internal Medicine, Saga University Faculty of Medicine, Saga, Japan.

Supported in part by the Research Grant for Cardiovascular Diseases (15C-1 and 18C-5) from the Ministry of Health, Labor and Welfare, Japan.

Disclosure: The authors report no conflicts of interest.

Received December 27, 2005. Accepted in final form March 29, 2006.

Address correspondence and reprint requests to Dr. Yusuke Yakushiji, Division of Neurology, Department of Internal Medicine, Saga University Faculty of Medicine, 5-1-1 Nabeshima, Saga 849-8501, Japan; e-mail: yakushiz@tg7.so-net.ne.jp

Commentary, see page 3

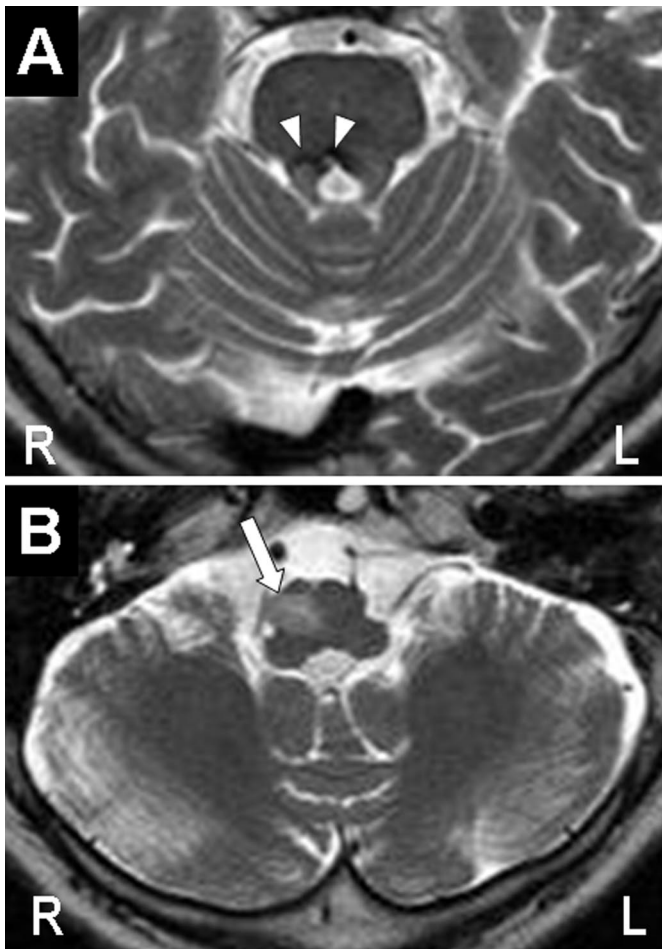


Figure 1. Brain T2-weighted MRI on admission. (A) Old small hemorrhage in the right pontine tegmentum (arrowhead). (B) The hypertrophic olive on the right side of the medulla (arrow).

quired myoclonic syndrome in adulthood.¹ The pathophysiologic mechanism of symptomatic ocular myoclonus remains largely unknown. Several potential candidates have been identified as generators of symptomatic ocular myoclonus, including the inferior olives,³ the nucleus ambiguus, and the dorsolateral reticular formation.⁴ Among them, the inferior olive, a member of the triangle of Guillain and Mollaret,⁵ is the most widely accepted. This hypothesis seems supported by the finding of increased rCMRGlucose levels throughout the medulla in patients with symptomatic palatal or oculopalatal myoclonus.²

In agreement with this observation,² we found an increased rCMRGlucose level in the hypertrophic olive before treatment of symptomatic ocular myoclonus. However, the increased rCMRGlucose level in the hypertrophic olive did not change even after symptomatic ocular myoclonus was alleviated by clonazepam, a reinforcer of GABAergic inhibition. Therefore, this result does not support the hypothesis that the hypertrophic olive acts as a generator of symptomatic ocular myoclonus.

The finding of an rCMRGlucose decrease in the inferior cerebellar vermis after the disappearance of symptomatic ocular myoclonus led us to conclude that the activity of the inferior cerebellar vermis is involved in the generation of symptomatic ocular myoclonus. The inferior cerebellar vermis, including the nodulus, which is a part of the vestibulocerebellar system, is associated with the vestibulo-ocular reflex (VOR), the optokinetic reflex, and the neck reflex.⁶ The vestibulocerebellar system has inputs that include primary or secondary vestibular fibers and mossy fibers originating in the pontine tegmental reticular nucleus. The dorsolateral reticular formation adjacent to the nucleus ambiguus has been

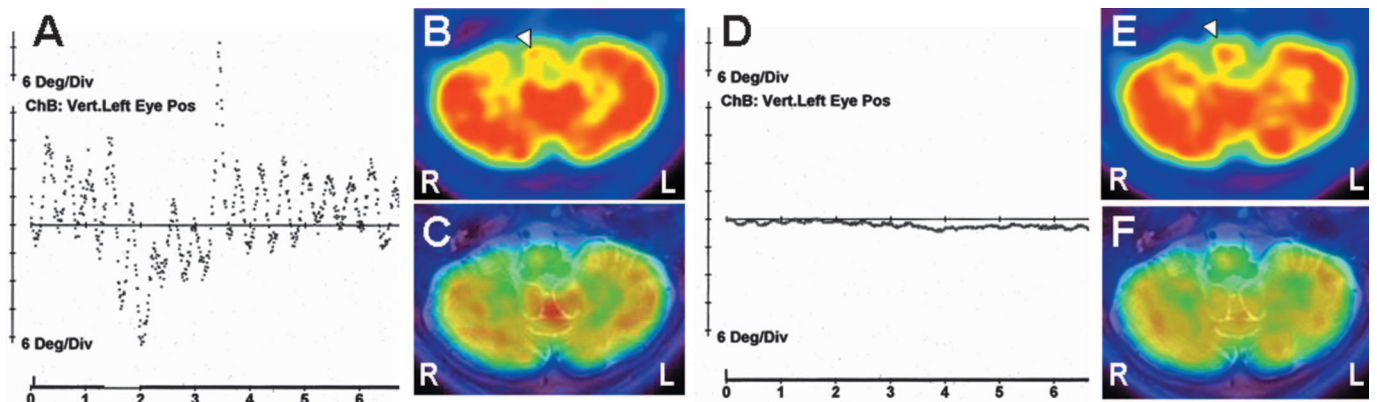
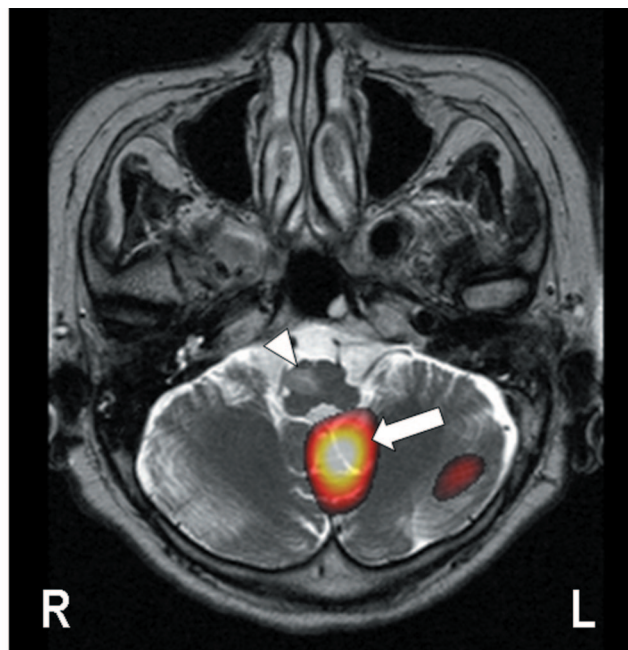


Figure 2. Electronystagmography (ENG) and PET with F-18 fluorodeoxyglucose (FDG-PET) performed before (day 0) and after (day 7) treatment of symptomatic ocular myoclonus. (A) ENG performed on day 0 shows a rhythmic, pendular, vertical ocular myoclonus at 2 to 3 cycles/second. (B) FDG-PET performed on day 0 shows increased regional cerebral metabolic rate of glucose use (rCMRGlucose) on the right side of the ventral medulla. (C) FDG-PET accumulation image of B is overlaid on the coregistered T2-weighted magnetic resonance (MR) image. (D) ENG performed on day 7 shows improvement of ocular myoclonus. (E) Follow-up FDG-PET performed on day 7 shows that increased rCMRGlucose on the right side of the ventral medulla remained. (F) FDG-PET image of E is overlaid on the coregistered T2-weighted MR image. Note that each FDG image on day 0 and day 7 is not presented in the same color range but is represented using an arbitrary color range.



(% decrease in Day 7, scaled by the global CMRGlucose)

Figure 3. A percent decrease of regional cerebral metabolic rate of glucose use (rCMRGlucose) (scaled by the global CMRGlucose) after day 7 compared with day 0, overlaid on the T2-weighted image. The area with the most decreased rCMRGlucose (-25%) level is located in the inferior cerebellar vermis (arrow) contralateral to the hypertrophic olive (arrowhead), whereas no significant decrease (less than -5%) in rCMRGlucose is found in the hypertrophic olive.

proposed as a candidate generator of palatal myoclonus.⁵

However, the hypermetabolism of the inferior cerebellar vermis may not be the result of neuronal activity generating symptomatic ocular myoclonus, but may be due to a secondary activity that is adapting to the presence of symptomatic ocular myoclonus. It has been postulated that the generation of ocular oscillation in symptomatic ocular myoclonus involves

VOR adaptation mediated by the floccus,⁷ which belongs to the vestibulocerebellar system. A recent study using a mathematical model hypothesized that while the jerky eye movement originates from the synchronized cell activity in the inferior olive, and the learning responses of the flocculus convert it into a smoother quasipendular motion that resembles symptomatic ocular myoclonus.⁸

The cause of the increased rCMRGlucose level in the hypertrophic olive of the current case needs to be determined. We would suggest that the increased rCMRGlucose in the hypertrophic olive may reflect a pathologic rather than a functional change. The pathologic changes in the hypertrophic olive consist of gliosis, including gemistocytic astrocytes, the enlargement and vacuolation of neurons, and demyelination.⁹ In fact, the number of astrocytes located in the hypertrophic olive was found to increase during a 2-year period after the onset of an interruption in the triangle of Guillain and Mollaret.¹⁰

Acknowledgment

The authors thank Dr. Yasuo Kuroda for helpful suggestions.

References

1. Tahmoush AJ, Brooks JE, Keltner JL. Palatal myoclonus associated with abnormal ocular and extremity movements: a polygraphic study. *Arch Neurol* 1972;27:431-440.
2. Dubinsky RM, Hallett M, Di Chiro G. Increased glucose metabolism in the medulla of patients with palatal myoclonus. *Neurology* 1991;41:557-562.
3. Matsuo F, Ajax ET. Palatal myoclonus and denervation supersensitivity in the central nervous system. *Ann Neurol* 1979;5:72-78.
4. Kane SA, Thach WT Jr. Palatal myoclonus and function of the inferior olive: are they related? In: Strata P, ed. *The olivocerebellar system in motor control. Experimental brain research series. Vol 17.* Berlin: Springer-Verlag, 1989:427-460.
5. Guillain G, Mollaret P. Deux cas de myoclonies synchrones et rythmées vélo-pharyngo-laryngo-oculo-diaphragmatiques. Le problème anatomique et physio-pathologique de ce syndrome. *Rev Neurol (Paris)* 1931;2:545-566.
6. Ito M. *The cerebellum and neural control.* New York: Raven, 1984.
7. Nakada T, Kwee IL. Oculopalatal myoclonus. *Brain* 1986;109:431-441.
8. Leigh RJ, Hong S, Zee DS, Optican LM. Oculopalatal tremor: clinical and computational study of a disorder of the inferior olive. *Soc Neurosci Abstr* 933.8 2005.
9. Goto N, Kaneko M. Olivary enlargement: chronological and morphometric analyses. *Acta Neuropathol (Berl)* 1981;54:275-282.
10. Nishie M, Yoshida Y, Hirata Y, Matsunaga M. Generation of symptomatic palatal tremor is not correlated with inferior olivary hypertrophy. *Brain* 2002;125:1348-1357.

Neurology[®]

Glucose utilization in the inferior cerebellar vermis and ocular myoclonus

Y. Yakushiji, R. Otsubo, T. Hayashi, et al.

Neurology 2006;67;131-133

DOI 10.1212/01.wnl.0000223837.52895.2e

This information is current as of July 10, 2006

Updated Information & Services	including high resolution figures, can be found at: http://www.neurology.org/content/67/1/131.full.html
References	This article cites 7 articles, 3 of which you can access for free at: http://www.neurology.org/content/67/1/131.full.html#ref-list-1
Citations	This article has been cited by 3 HighWire-hosted articles: http://www.neurology.org/content/67/1/131.full.html#otherarticles
Permissions & Licensing	Information about reproducing this article in parts (figures, tables) or in its entirety can be found online at: http://www.neurology.org/misc/about.xhtml#permissions
Reprints	Information about ordering reprints can be found online: http://www.neurology.org/misc/addir.xhtml#reprintsus

Neurology® is the official journal of the American Academy of Neurology. Published continuously since 1951, it is now a weekly with 48 issues per year. Copyright . All rights reserved. Print ISSN: 0028-3878. Online ISSN: 1526-632X.

